

Modification of size and magnetic properties of implanted Co nanoparticles by irradiation

C. D'Orléans^{1,2}, J. J. Grob, D. Muller, J. P. Stoquert

¹*Laboratoire PHASE (UPR 292 CNRS), 23 Rue du Loess, 67037 Strasbourg, FRANCE*

C. Estournès, J. L. Guille, M. Richard-Plouet

²*IPCMS-GMI (UMR 75040 CNRS), 23 Rue du Loess, 67037 Strasbourg, FRANCE*

C. Cerruti, F. Haas

IReS (UMR 7500 IN2P3 - CNRS), 23 Rue du Loess, 67037 Strasbourg, FRANCE

Cobalt ions have been implanted in amorphous silica layers on Si wafers at an energy of 160 keV and at three different fluences ($2 \cdot 10^{16}$, $5 \cdot 10^{16}$ and 10^{17} at.cm⁻²). Magnetic properties of implanted Co have been measured with a SQUID magnetometer at 295 K and 5 K and shape and size of the nanoparticles have been studied by Transmission Electron Microscopy (TEM). Various post-implantation thermal treatments performed at different temperatures, for different duration and under neutral or reducing atmospheres do not modify the cobalt particle size. Post-implantation irradiations with swift heavy ions of implanted samples change the particle size and under higher irradiation fluence changes the shape.

Introduction

Metallic materials with nanometer-scale particles may be used in numerous applications (optical, micromechanical and information storage devices)¹. Metallic nanoparticles show properties significantly different from those observed in the bulk material. Nanoparticles can be prepared by physical methods (inert gas evaporation, sputtering, laser vaporization)^{2,3}, or by chemical methods (sol-gel, inverse micelle technique)^{4,7}.

Concerning magnetic materials, several specific features related to nanometer size have been reported such as enhanced magnetization⁸, anisotropy, coercivity and dipolar interactions⁹. An important challenge in understanding these phenomena is to have well defined samples with controllable size and inter-particle distance. It has been recently shown that the use of an inorganic matrix like glasses or a SiO₂ xerogel^{10,11} is a good host for crystalline metallic nanoparticles. However, due to the low solubility of transition metals in these matrices, only a low volume fraction can be obtained in the form of monolithic samples.

Ion implantation is becoming a powerful technique for synthesizing nano-particles embedded in amorphous insulating matrix in order to create composite materials with interesting optical and magnetic properties¹².

Amorphous silica samples have been implanted at different fluences and at different temperatures; post-implantation treatments made on these implanted samples, such as thermal annealings and heavy ion irradiations, have been studied. Cobalt implanted silica layers have been characterized by magnetic measurements and microscopy (TEM).

Experimental procedures

A silica layer resulting from the thermal oxidation of a silicon substrate has been implanted with cobalt ions at an energy of 160 keV. Different implantation fluences ($2 \cdot 10^{16}$, $5 \cdot 10^{16}$ and 10^{17} Co⁺.cm⁻²) have been implanted at temperatures of 77 K, 295 K and 873 K.

Different thermal treatments have been performed on implanted samples: samples under argon atmosphere for 2h to set temperatures between 473 K and 973 K; they have been held at the set temperature for times varying from 1h to 10h under neutral (argon) or reducing (hydrogen) atmosphere, then they have been allowed to cool down to room temperature under argon flow.

Post-implantation irradiations have also been made with swift heavy ions at the Vivitron Accelerator in Strasbourg. Implanted samples have been irradiated with ^{127}I ions at 200 MeV at room temperature and at fluences of 10^{11} and 10^{13} ions.cm⁻².

The profile of the implanted species in the substrate has been determined by Rutherford Backscattering Spectroscopy (RBS) with an analyzing beam of $^4\text{He}^+$ at an energy of 2 MeV at a scattering angle of 120°.

A Superconducting Quantum Interference Device magnetometer (SQUID) was used to measure the magnetic properties of the implanted samples at 295 K and 5 K to a maximum field of 5 T. All quoted magnetisation are expressed as magnetic moment per area of substrate.

High Resolution Transmission Electron Microscopy (HRTEM Topcon EM002B) observations were made on thinned hand-polished cross-sectional specimen, applying an acceleration voltage of 200 kV.

Results

RBS measurements have been used to control the depth profile of the specie implanted in the samples. The profile of the cobalt concentration is Gaussian, and for implantation made at an energy of 160 keV, the projected range is about 95 nm for any implantation fluence. The depth profile of implanted cobalt is not modified with the post-implantation treatments.

Dose Effect

Samples have been implanted at three different fluences $2 \cdot 10^{16}$, $5 \cdot 10^{16}$ and 10^{17} at.cm⁻². For a given implantation temperature, the particle size is not modified with the implantation fluence. Therefore, only the density of particles increases, and the inter-particle distance decreases with the implantation dose. However, for the implantation of $2 \cdot 10^{16}$ at.cm⁻² made at 77 K, particles are smaller, and the distance between them being larger, it is difficult to observe them with TEM.

Implantation Temperature Effect

Figure 1 shows the effect of the implantation temperature on particle size. For a sample implanted at 10^{17} at.cm⁻², the mean diameter D_0 increases from 3.5 nm for samples implanted at 77 K, to 4.8 nm for implantations made at room temperature¹³ and to 8 nm for implantations made at 873 K.

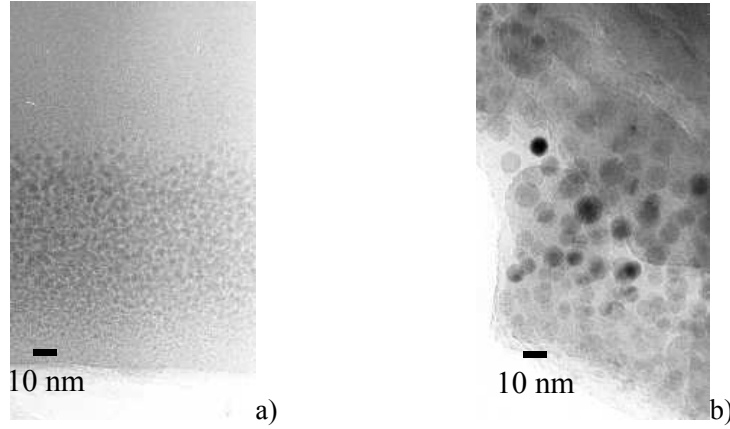


Fig 1: TEM images of samples implanted a) at 77 K ($D_0 = 3.5$ nm) and b) at 873 K ($D_0 = 8$ nm)

Annealing Effect

Thermal treatments have been performed on samples implanted at 77 K at 10^{17} at.cm⁻². Annealing made at temperatures varying from 473 K to 973 K for times varying from 1h to 10h and under neutral atmosphere do not change particle size. For annealing made under hydrogen atmosphere at a temperature of 873 K for 7h, the mean diameter of the particles is not modified, but the particles that are not in the form of metallic cobalt are reduced, as suggested by the increase in magnetisation at saturation (figure 2) ¹³.

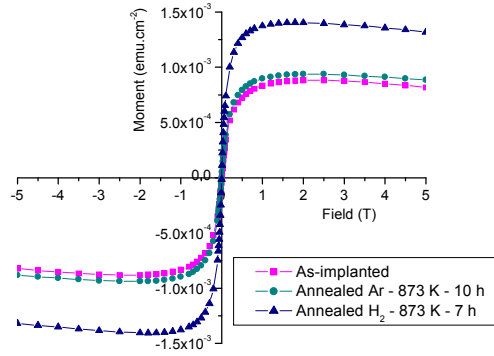


Fig 2: Magnetic moment as a function of the applied field at 295 K for an as-implanted sample, for a sample annealed under argon atmosphere at 873 K for 10 h, and for a sample annealed under hydrogen atmosphere at 873 K for 7 h.

Irradiation Effect

First, irradiations have been carried out with electrons at 200 kV in the Transmission Electron Microscope. As seen in figure 3 a), for a sample implanted at 10^{17} at.cm⁻² at 77 K, particles are not modified with electron irradiation at room temperature (normal conditions for observation). Particles are growing during the observation when the same sample is heated in the following way: it is first heated for 1h to a temperature of 873 K while exposing a selected area to electron irradiation, and then maintained at 873 K for 2h, and finally cooled down to room temperature in 30 minutes without electron exposure. After two hours, the mean diameter is still about 3.5 nm for particles non exposed to electron beam, and for particles exposed to electrons, their mean diameter has reached a maximum size of 50 nm as shown in figure 3 b).

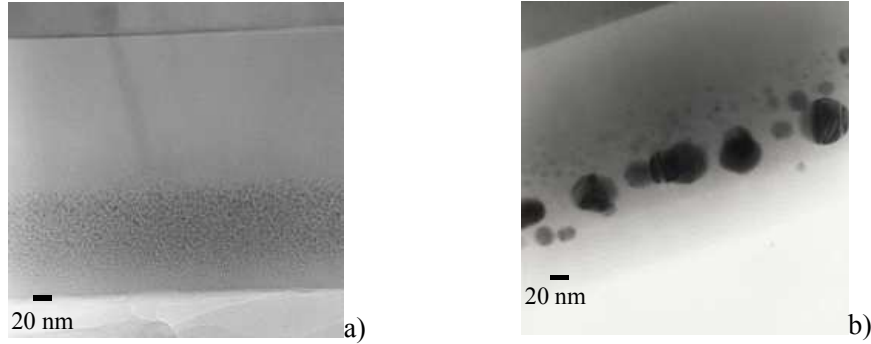


Fig 3: TEM images of samples observed a) at room temperature and b) at 873 K

Irradiations at room temperature with ^{127}I ions at 200 MeV (10^{11} and 10^{13} ions. cm^{-2}) have been made on samples implanted at 873 K at a fluence of 10^{17} at. cm^{-2} and for which the mean diameter of the particles is 8 nm. Figure 4 shows that the saturation magnetization is not changed with post-implantation irradiations, but the coercive fields measured at 5 K increase with the irradiation dose, which suggests an increase in particle size ¹⁴.

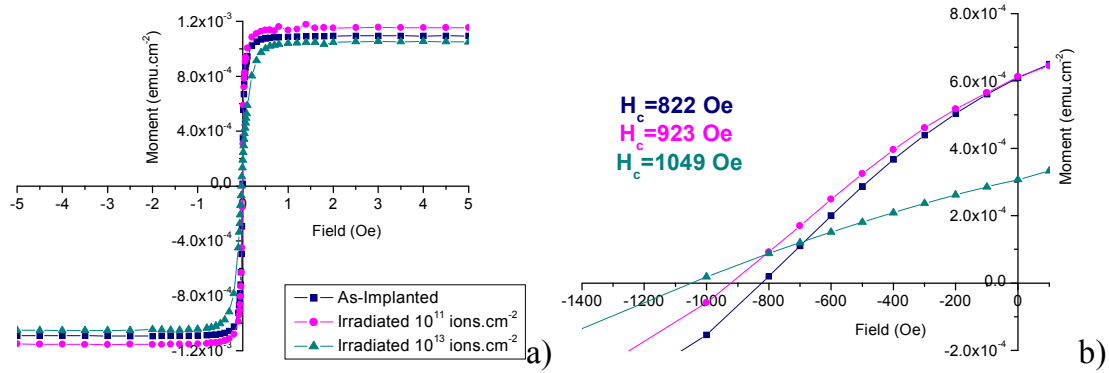


Fig 4: a) Magnetic moment measured as a function of the applied field at 295K, and b) coercive fields at 5K for samples implanted at 10^{17} at. cm^{-2} at 873 K and irradiated at 10^{11} and 10^{13} ions. cm^{-2}

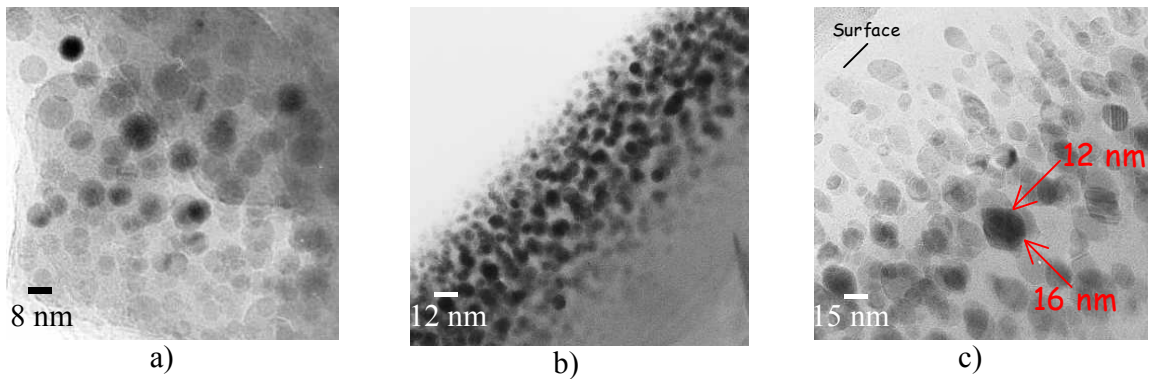


Fig 5: TEM images of a) 873 K implanted samples and irradiated b) at 10^{11} and c) at 10^{13} ions. cm^{-2} .

As seen in figure 5, TEM observations confirm that particle size and even particle shape are modified by irradiation. The mean diameter of the particles increases from 8 nm to 12

nm for the implanted sample irradiated at 10^{11} ions.cm⁻²; for the irradiation at 10^{13} ions.cm⁻², particles are stretched in the irradiation direction: the mean diameter is still 12 nm in the direction parallel to the surface, and 16 nm in the perpendicular direction.

Conclusion

This study shows the dependence of particle size on the implantation temperature for a given implantation fluence. The mean diameter of nanoparticles is not modified if we apply only thermal treatments or only electron irradiations. However, particle size changes for electron irradiation at 873 K and for irradiation with swift heavy ions. Noting that ion irradiation induces local electronic excitation and temperature increase, we see that in both cases, the change of particle size necessitates both the electronic and thermal contributions.

¹ A. Meldrum, R.F. Haglund Jr., L.A. Boatner and C.W. White, Adv. Mater. **13** (2001) 1431.

² W. Gong, H. Li., Z. Zhao, and J. Chen, J. Appl. Phys. **69** (1991) 5119.

³ S. Honda, T. Okada, N. Nawate and M. Tokumoto, Phys. Rev. B **56** (1997) 14566.

⁴ T. Lutz, C. Estournès, and J.L. Guille, J. of Sol-Gel Science and Technology **13** (1998) 929.

⁵ F. Schweyer, C. Estournès, M. Richard, J. L. Guille, J. Rosé, P. Braunstein, J. L. Paillaud and H. Kessler, Chem. Commun. **14** (2000) 1271.

⁶ T. Ould Ely, C. Amiens, B. Chaudret, E. Snoeck, M. Verlest, M. Respaud and J.M. Broto, Chem. Mater. **11** (1999) 526.

⁷ J.S. Jung, W.S. Chae, R.A. McIntyre, C.T. Seip, J.B. Wiley and C.J.O'Connor, Mat. Res. Bull. **34** (1999) 1353.

⁸ J.P. Chen, C.M. Sorensen, K.J. Klabunde and C.G. Hadjipanayis, Phys. Rev. B **51** (1995) 11527.

⁹ R.H. Kodama, J. Mag. Mag. Mat. **200** (1999) 359.

¹⁰ C. Estournès, T. Lutz and J. L. Guille, J. Non-Cryst. Solids **197** (1996) 192.

¹¹ C. Estournès, T. Lutz, J. Happich, T. Quaranta, P. Wissler and J. L. Guille, J. Mag. Mag. Mat. **173** (1997) 83.

¹² O. Cintora-Gonzalez, C. Estournès, J.L. Guille, D. Muller and J.J. Grob, Nucl. Inst. And. Meth. B **147** (1999) 422.

¹³ O. Cintora-Gonzalez, C. Estournès, D. Muller, M. Richard-Plouet, A. Traverse, J.L. Guille and J.J. Grob, Mat. Res. Soc. Symp. Proc. **647**, (2001) O5.12.1.

¹⁴ A. Herpin, Théorie du magnétisme Presse Universitaire de France(1968).